Mathematical modeling and simulation of a diolefin saturation reactor used in a naphtha hydrotreating process

(iD) Marteson Cristiano dos Santos Camelo [1]*

(iD) Sérgio Lucena [2]

(iD) Rony Glauco de Melo [3]

[1] marteson.camelo@ufape.edu.br
Universidade Federal do Agreste de Pernambuco (UFAPE), Campus Garanhuns, Brazil

[2] slucena@gmail.com
Departamento de Engenharia Química, Universidade Federal de Pernambuco (UFPE), Brazil

[3] ronymelo@recife.ifpe.edu.br
Instituto Federal de Educação, Ciência e Tecnologia de Pernambuco (IFPE), Campus Recife, Brazil

*Corresponding author.

ABSTRACT: This paper describes a dynamic mathematical model developed to simulate a diolefin reactor currently used in an existing naphtha hydrotreating process. Diolefins polymerize at temperatures above 200 °C, which is reached in a reactor of hydrotreatment of naphtha. Therefore, the diolefins must be removed before they reach the hydrotreating reactors. This hydrotreating unit has an essential role in modern refineries as it specifies the naphtha of different units, such as distillation and delayed coker. A mathematical model of a three-phase reactor was developed. It was used to obtain the kinetics of the diolefin and olefin saturation reaction in a temperature range of 180 ºC to 200 °C, and pressure of 3.5 MPa to 4 MPa. The kinetic model was developed from the experimental data from a Brazilian refinery. The reactor model includes correlations for determining mass-transfer coefficients, kinetics reaction rates, and properties of the compounds under process conditions. The kinetic model predicted the temperature profile along the reactor length with a minor absolute error. The developed model offers reliable simulated results when compared to experimental data.

Keywords: kinetics of diolefin saturation; mathematical modeling; naphtha hydrotreating.

Modelagem matemática e simulação de um reator de saturação de diolefinas utilizado em um processo de hidrotratamento de nafta

RESUMO: *Este trabalho apresenta um modelo matemático desenvolvido para simular um reator de saturação de olefinas presente em um processo de hidrotratamento de nafta. As diolefinas polimerizam em temperaturas acima de 200 °C, que é alcançada em um reator de hidrotratamento de nafta. Portanto, as diolefinas devem ser removidas da corrente de entrada do reator de*

hidrotratamento. A unidade de hidrotratamento de nafta tem papel importante nas refinarias modernas, uma vez que estas são responsáveis pela especificação da nafta oriunda de diferentes unidades, como a destilação e o coqueamento retardado. Um modelo matemático de um reator trifásico foi desenvolvido e utilizado para obter a cinética de saturação das olefinas e diolefinas na faixa operacional de temperatura entre 180 °C e 200 °C e pressão entre 3,5 Mpa e 4 Mpa. O modelo cinético desenvolvido neste trabalho foi obtido através de dados experimentais de uma refinaria brasileira. O modelo do reator inclui correlações para determinação dos coeficientes de transferência de massa, taxa cinética de reação e propriedades dos componentes presentes na alimentação do reator sob condições de processo. O modelo cinético foi capaz de predizer o perfil de temperatura do reator com um valor baixo de erro. O modelo desenvolvido fornece resultados simulados compatíveis com os resultados experimentais.

1 Introduction

Naphtha is a light oil product usually coming from crude oil atmospheric distillation and other streams (Ex. delayed coking unit). The naphtha produced in this process contains both olefins and diolefins compounds and a high content of contaminants, such as sulfur and nitrogen compounds. The contents of sulfur and nitrogen can vary, respectively, 1.44-1.60 wt% and 0.18-0.25 wt%, while the contents of olefin and diolefin can vary 31.7-36.6 wt% and 4.2-4.4 wt%, respectively (YUI, 1999). Due to environmental restrictions, the legislation preconizes that sulfur and nitrogen contents must be reduced; in addition, the olefin concentration in naphtha must be adjusted to attending to the market specifications.

Hydrotreating is the main process used in oil refineries to treat streams rich in sulfur and nitrogen. Through this process, it is possible to attend to the environmental restrictions applied to automotive fossil fuels by reducing the number of pollutants. The process operating conditions depend on the type of oil fraction treated. As an example, naphtha hydrotreating operates in less severe pressure and temperature conditions (T = 200 °C, P = 35 bar) than the diesel hydrotreating conditions (T = 380 °C, P = 45 bar) (ANCHEYTA, 2011).

Naphtha hydrotreating can vary according to the refining scheme: usually, the process uses two reactors in series; however, in some cases, three reactors can be used. The reactions are highly exothermic, so each reactor is divided into two or three catalyst beds. A low-temperature hydrogen stream is added between the catalyst beds to cool down the system. Figure 1 shows a simple flowchart of the hydrotreatment naphtha process.
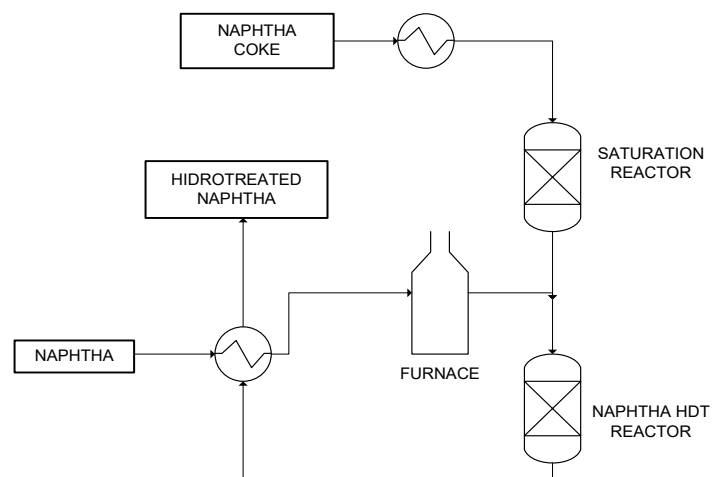
In the first reactor of the naphtha hydrotreatment unit occurs the pretreatment, the primary reaction in this process is the diolefin saturation, which yields olefins. This reactor has high relevance in naphtha hydrotreating, especially when the naphtha comes from the delayed coking unit due to the high contents of olefins and diolefins. The pretreatment reactor is a three-phase reactor containing gas, liquid, and solid phase. The operating temperature range is 180 ºC to 220 ºC. Keeping the temperature in this range is relevant to avoid the diolefin polymerization reaction (XIN *et al*., 2018).

The second reactor of the process is often referred to as the hydrotreating reactor; it is the main reactor responsible for removing sulfur and nitrogen compounds from the feed stream. The operational conditions of the hydrotreating reactor are more severe than the diolefin reactor. Therefore, the concentration of diolefins in the feed stream must be low; otherwise, the diolefins can polymerize, resulting in catalyst contamination. Usually, the naphtha hydrotreating reactors are used as catalyst NiMo or CoMo supported by alumina (XIN *et al.*, 2018; YUI, 1999).

The fixed bed reactor modeling for the simulation of the hydrotreating process can be found in many papers in the literature (ANCHEYTA, 2011; BHASKAR *et al*., 2004; JIMÉNEZ; KAFAROV; NUÑEZ, 2007; KORSTEN; HOFFMANN, 1996; MEDEROS; ANCHEYTA, 2007; TOLEDO *et al*., 2008). All these papers presented the hydrotreatment process of medium distillate. However, few papers analyze naphtha hydrotreating (YUI, 1999; YUI; CHAN, 1992). For example, Yui (1999) showed that the kinetics of hydrodesulfurization (HDS), hydrodenitrogenation (HDN), and hydrogenation reactions of diolefins, olefins, and aromatics were fitted by a pseudo-first-order model. Furthermore, they showed that the only reaction that occurred significantly below 200 °C was the olefin hydrogenation; the others occurred significantly above 200 °C.

Olefin/diolefin reaction kinetic models have been studied in references as Toba *et al*. (2007) studied the reactions of olefin and sulfur compounds from the FCC unit. According to their results, the olefin conversion is affected by double bond location and the presence of methyl groups. In the same way, Badawi, Vivier and Duprez (2010) studied the influence of different types of catalysts in the kinetic model in the FCC unit. Xin *et al*. (2018) studied the olefin hydrogenation in derived naphtha from bitumen, it was determined that the diolefins are more reactive than olefins, and the temperature has a significant effect on olefin hydrogenation performance, while the parameters pressure and the liquid hourly space velocity have moderate effects.

As the mathematical models of the naphtha hydrotreating reactor are unpublished in the literature, this work intends to develop a mathematical model for this process. The

main objective is to develop a mathematical model for the naphtha hydrotreating reactor and simulate it using the operational conditions under the diolefin reactor in dynamic conditions. It could be used to study the process of dynamic behavior, as well as serve as a predictive model to process control. Besides, a kinetic model for the olefins and diolefins saturation reactions was obtained suitable for the naphtha hydrotreatment process.

2 Methodology

This section shows all the assumptions made to obtain a mathematical model for the diolefin saturation reactor and the operational conditions applied to simulate the reactor.

2.1 Reaction kinetics

Although the reactor feedstock contains sulfur, nitrogen, and hydrocarbons, only the saturation reactions of diolefins and olefins were considered since the other reactions need severe conditions (YUI, 1999; YUI; CHAN, 1992). In these reactions, hydrogen is directed to break a double bond, as shown in Equation 1 and Equation 2.

$$R = C = CH_2 + H_2 \xrightarrow{k_{dio}} R - CH = CH_2 \tag{1}$$

$$R - CH = CH_2 + H_2 \xrightarrow{k_{ole}} R - CH_2 - CH_3 \tag{2}$$
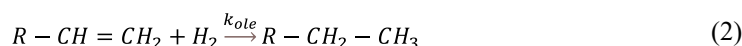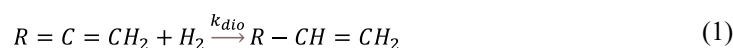
The nature of the olefin and the diolefin saturation reaction is similar because a first-order kinetic model was adopted, as listed in Equations 3-5. This model has assumed that it is no competition between olefins and diolefins with other naphtha components by the catalytic site because the reactions of hydrodesulfurization and hydrodenitrogenation are more effective in temperatures higher than those applied in this paper, as reported in Yui (1999) and Dukanovic *et al.* (2013). Therefore, the reaction rate constant was calculated by Equation 5.

$$r_{ole} = k_{ole} C_{ole}^S \tag{3}$$

$$r_{dio} = k_{dio} C_{dio}^S \tag{4}$$

$$k_j = k_j^0 e^{-e_{aj}/RT_s} \tag{5}$$

The reaction parameters (the kinetic constant and the activation energy) were estimated by the process data from a Brazilian refinery. In addition, they provided the profile of temperature and diolefin concentration along the reactor. In this process, the diolefin reactor has used $NiMo/Al_2O_3$ as catalyst. The temperature profile is shown in Table 1. From these data, the reaction parameters were determined using a range of temperature between 180 ºC to 200 °C. Although the local optimization techniques can achieve an adequate kinetics data fit, these were not used in this work. Genetic algorithms were used because the search space is not restricted to local optima (LINDEN, 2012).

The objective function used to determine the kinetic parameters of the saturation reactions is shown in Equation 6.

$$\sum_{i=1:n} \left(T_{exp} - T_{sim}\right)^2 \tag{6}$$

where: T_{exp} is the experimental temperature; T_{sim} is the temperature obtained by the mathematical model.

z (m)	Temperature (°C)
0	180
0.8	181
3.3	185
4.2	185
5.0	186
5.8	188
6.7	189
7.5	191

2.2 Mathematical model of the diolefin reactor

Due to the less severe operational conditions, the diolefin hydrogenation reactor differs from the second reactor (the hydrotreating reactor). In this reactor, there are three phases:

- Gas phase: This phase is usually composed of hydrogen, but it can also have a small number of short-chain hydrocarbons;

- Liquid phase: it is composed of naphtha;

- Solid phase: it is the catalyst bed.

The assumptions used to build a mathematical model for the diolefin reactor are:

- The reactor operates under a transient/dynamic condition;

- Gas and liquid streams are concurrent flows;

- The gas and liquid velocities remain constant along the reactor;

- There are no radial concentration and temperature gradients;

- The catalyst activity remains constant over time;

- There is neither vaporization nor condensation of naphtha;

- The reactor works under constant pressure and adiabatic conditions;

- The chemical reactions occur on the catalyst surface only;

- The vapor-phase mass-transfer resistance was ignored;

- As the reactor operates on an industrial scale, the gas velocity and the liquid flows are high; thus, the axial dispersion was ignored;

- The gas-phase energy balance was ignored because the gas-phase heat capacity is much lower than the liquid-phase heat capacity.

2.3 Mass balance

The mass balance equations in the trickle bed reactor for the saturation processes of olefin and diolefin are described by the following set of differential Equations 7-10. The negative signal in the convective term indicates that the naphtha and the H_2 are in concurrent flows.

The only component in the gas phase is H_2. The H_2 mass balance differs from the other components due to the mass transfer from the gas to the liquid phase. The H_2 mass balance in the gas and liquid phases is described by Equation 7 and Equation 8, respectively.

$$
\begin{aligned}
\frac{\varepsilon_G}{RT_G}\frac{\partial p_{H_2}^G}{\partial t} &= -\frac{u_G}{RT_G}\frac{\partial p_{H_2}^G}{\partial z}\cdots \\
&\quad -k_{H_2}^L a_L\left(\frac{p_{H_2}^G}{H_{H_2}}-C_{H_2}^L\right)
\end{aligned}
\tag{7}
$$

$$
\begin{aligned}
\varepsilon_L\frac{\partial C_{H_2}^L}{\partial t} &= -u_L\frac{\partial C_{H_2}^L}{\partial z}+k_{H_2}^L a_L\left(\frac{p_{H_2}^G}{H_{H_2}}-C_{H_2}^L\right)\cdots \\
&\quad -k_{H_2}^S a_S\left(C_{H_2}^L-C_{H_2}^S\right)
\end{aligned}
\tag{8}
$$

In Equation 8, the last term on the right side represents the H_2 in the liquid phase absorbed into the solid phase. This term also is in Equation 9, which describes the mass balance equation for olefin and diolefin in the liquid phase.

$$
\varepsilon_L\frac{\partial C_i^L}{\partial t}=-u_L\frac{\partial C_i^L}{\partial z}-k_i^S a_S\left(C_i^L-C_i^S\right)
\tag{9}
$$

The surface concentration is obtained by the solid phase mass balance described by Equation 10, in which the compound "i" can be either hydrogen, olefin, or diolefin. The signal of the reactional term indicates compound consumption or compound production. For the reagents (hydrogen and diolefin), this term is negative, whereas the term is positive for the products (the olefin).

$$
\varepsilon_p(1-\epsilon)\frac{\partial C_i^S}{\partial t}=k_i^S a_S\left(C_i^L-C_i^S\right)\pm\rho_B r_j
\tag{10}
$$

2.4 Energy balance

According to Mederos and Ancheyta (2007), the liquid and solid energy balances are enough to describe the heat transfer phenomenon as the gas phase heat capacity is much lower than the liquid phase heat capacity. Equation 11 and Equation 12 represent the energy balances for the liquid and solid phases. As seen in Equation 12, the energy is added in the solid phase by two mechanisms: the thermal convection between liquid and solid phases and the saturation reaction, which is exothermic.

$$\varepsilon_L \rho_L c_{pL} \frac{\partial T_L}{\partial t} = -u_L \rho_L c_{pL} \frac{\partial T_L}{\partial z} \dots$$
$$-h_{LS} a_S (T_L - T_S)$$
(11)

$$\rho_S c_{pS}(1 - \epsilon) \frac{\partial T_S}{\partial t} = h_{LS} a_S (T_L - T_S) \dots$$
$$\pm \rho_B \sum_j r_j (-\Delta H_{Rj})$$
(12)

2.5 Simulation of the mathematical model of the diolefin reactor

The reactor model parameters, such as heat and mass transfer coefficients, gas solubility, and properties of gases and oil under process conditions, were estimated by the correlations identified in the literature (KORSTEN; HOFFMANN, 1996; MEDEROS; ANCHEYTA, 2007), which are presented in Table 2.

Table 2 ►
Correlations used to estimate parameters of the model.
Source: Korsten and Hoffmann (1996); Mederos and Ancheyta (2007)

Parameter	Correlation
Oil viscosity (mPa s)	$\mu_L = 3.141 x 10^{10}(T_L - 460)^{-3.444}[\log_{10}(API)]^a$ $a = 10.313[\log_{10}(T_L - 360)] - 36.447$
Gas-liquid mass transfer coefficient (cm/s)	$\dfrac{k_L^i}{D_L^i} = 7\left(\dfrac{D_L}{\mu_L}\right)^{0.4}\left(\dfrac{\mu_L}{D_L^i \rho_L}\right)^{0.5}$
Liquid-solid mass transfer coefficient (cm/s)	$\dfrac{k_S^i}{a_S D_L^i} = 1.8\left(\dfrac{G_L}{\mu_L a_S}\right)^{0.5}\left(\dfrac{\mu_L}{D_L^i \rho_L}\right)^{1/3}$
Molecular diffusivity (cm²/s)	$D_L^i = 8.93 x 10^{-8}\left(\dfrac{v_L^{0.267}}{v_i^{0.433}}\right)\left(\dfrac{T_L}{\mu_L}\right)$
Molar volume (cm³/mol)	$v_i = 0.285 v_c^{1.048}$ $v_c^m = 7.5214 x 10^{-3}(T_{MBP}^{0.2896})(d_c^{-0.7666})$
Henry's coefficient (MPa.cm³/mol)	$H_{H_2} = \dfrac{v_N}{\lambda_i \rho_L}$
Solubility coefficient H₂ Nl/(MPa kg)	$\lambda_{H_2} = -0.559729 - 0.42947 x 10^{-3}T_L + 3.07539 x 10^{-3}\left(\dfrac{T_L}{\rho_{20}}\right) + 1.94593 x 10^{-6}T_L^2 \dots$ $+ \dfrac{0.835783}{\rho_{20}^2}$
Oil density (lb/ft³)	$\rho(P,T) = \rho_0 + \Delta\rho_P + \Delta\rho_T$ $\Delta\rho_P = [0.167 + (16.181 x 10^{-0.0425\rho_0})]\left(\dfrac{P}{1000}\right) \dots$ $-0.01[0.299 + (263 x 10^{-0.0603\rho_0})]\left(\dfrac{P}{1000}\right)^2$ $\Delta\rho_T = [0.0133 + 152.4(\rho_0 + \Delta\rho_P)^{-2.45}](T - 520) \dots$ $-\left[8.1 x 10^{-6} - 0.0622 x 10^{-0.764(\rho_0 + \Delta\rho_P)}\right](T - 520)^2$

Table 3 contains the geometric reactor parameters used in the simulation and the naphtha feedstock composition (BHASKAR *et al.*, 2004; MEDEROS; ANCHEYTA, 2007). These data are similar to those from the refinery that provided the experimental data for the kinetic study.

Parameters	Value
L_t (m)	7.5
D_R (m)	2.0
P (MPa)	3.9
T_0 (K)	453
Feed flow rate (m³/d)	3000
Ratio H_2/naphtha (Nm³/m³)	763
d_c (m)	2.54×10^{-3}
$API°$	57
PM_{oil} (g/mol)	120
T_{MBP} (K)	469.80
Nitrogen ppm	200
Sulfur ppm	2
Olefins wt%	22.57
Diolefins wt%	6
Gas composition of H_2	100%

The partial differential equations that describe the model were transformed into a set of first-order ordinary differential equations by the method of backward finite difference, Equation 13. Thus, the coordinate axial "z" was discretized and the reactor was divided into ten points. The resulting system was written in Matlab® 2014 computational code and was solved by using the ODE15s Matlab® package, this routine uses Gear's method to solve the system of differential equations. The Gear's method generally is indicated to solve stiff problems, as an example, some mathematical models used to model chemical processes:

$$\frac{dC}{dz} = \frac{C_m - C_{m-1}}{\Delta z} \qquad \text{13)}$$

2.5.1 Boundary and initial conditions

The initial and boundary conditions are shown in Table 4. The oil at the reactor inlet was considered initially saturated with hydrogen. Besides, the hydrogen stream in the inlet has high purity. At the reactor inlet, the temperatures of liquid and solid phases are equal to the feedstock temperature.

$t = 0$		
	$z = 0$	$\begin{cases} p_{H_2} = P_T \\ T_L = T_S = T_0 \\ C_{L,i} = C_i^0 \quad i = dio, ole, H_2 \\ C_{s,i} = 0 \quad i = dio, ole, H_2 \end{cases}$
	$0 < z \le L$	$\begin{cases} p_{H_2} = P_T \\ T_L = T_S = T_0 \\ C_{L,i} = 0 \quad i = dio, ole, H_2 \\ C_{s,i} = 0 \quad i = dio, ole, H_2 \end{cases}$
$t > 0$		
	$z = 0$	$\begin{cases} p_{H_2} = P_T \\ T_L = T_S = T_0 \\ C_{L,i} = C_i^0 \quad i = dio, ole, H_2 \\ C_{s,i} = 0 \quad i = dio, ole, H_2 \end{cases}$

3 Results

Through the optimization study, the reaction rate was found (these results are in Table 5). The reaction rate of diolefin saturation is higher than the olefin saturation rate when the temperature is below 200 °C, as related by Yui (1999). The reactor of diolefin and olefin hydrogenation was simulated, with the kinetic model obtained. The operational conditions, geometric reactor parameters, and naphtha composition used in the simulation are in Table 3.

Parameter	Value
k_{ole}^0	5.775×10^2 m³/(kg.s)
k_{dio}^0	8.297×10^2 m³/(kg.s)
e_{ole}	1.135×10^5 J/mol
e_{dio}	7.423×10^4 J/mol

Although the naphtha feedstock has sulfur and nitrogen in its composition, these compounds do not affect the behavior of the reactor since the kinetic model developed does not take into account the competitive effect of sulfur and nitrogen at the olefin and diolefin hydrogenation reaction. That is suitable for the temperature range studied between 180 ºC and 200 °C, equal to the operational condition applied to the reactor of diolefin and olefin hydrogenation, since the optimal temperature of the reactions of hydrodesulfurization and hydrodenitrogenation is above 200 °C, as reported at Yui (1999) and Dukanovic *et al*. (2013).

Figure 2 shows the liquid phase temperature along the catalytic bed; as can be seen, the adjustment between the model outlet and the experimental data is satisfactory, with a mean absolute error of 0.32.
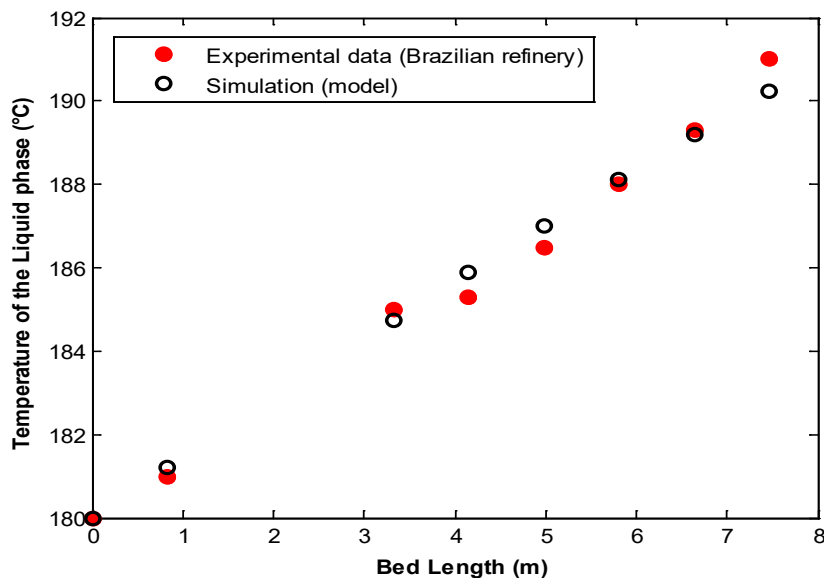
In Figures 3 and 4, it is shown, respectively, the profile for the diolefin and olefin concentrations in the liquid phase at different points in the reactor along the time. It was simulated at a time of 600 s to observe the dynamic behavior at the reactor startup. Due to the reactants' residence time in the catalyst bed, further away from the reactor inlet, the longer the time to reach a steady state. Therefore, the diolefin concentration reaches a steady state in the 200 s at the outlet of the reactor. The diolefin hydrogenation reactions break one double bond of this compound, ending up in olefins. As shown in Figure 3, the diolefin concentration decreases along the reactor length. It reaches a conversion of about 42%. This conversion is below the result shown in Xin *et al*. (2018), which showed a conversion of diolefin next to 100%, at 180 °C, and LHSV equal to 1.5 h^{-1}. It matches the lower flow rate applied in the presented work. The increase in flow rate decreases the diolefin conversion, resulting from a decrease in the residence time of reactants in the reactor (XIN *et al*., 2018).
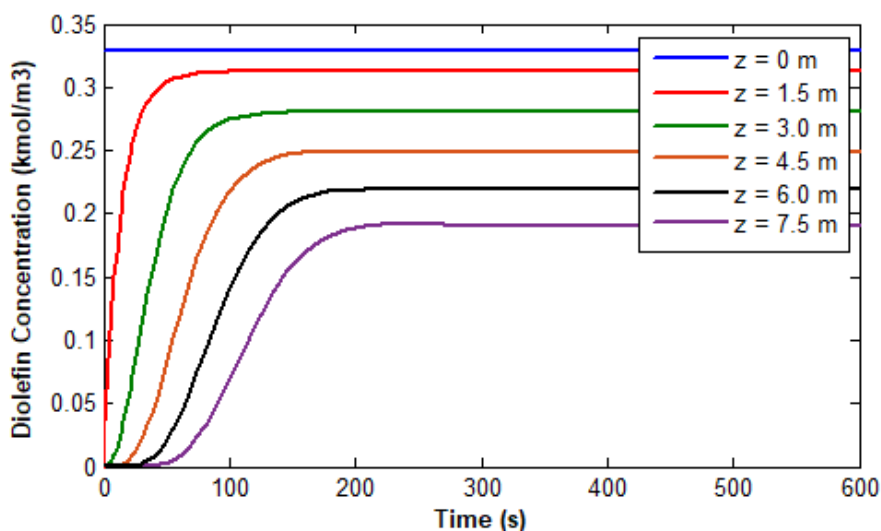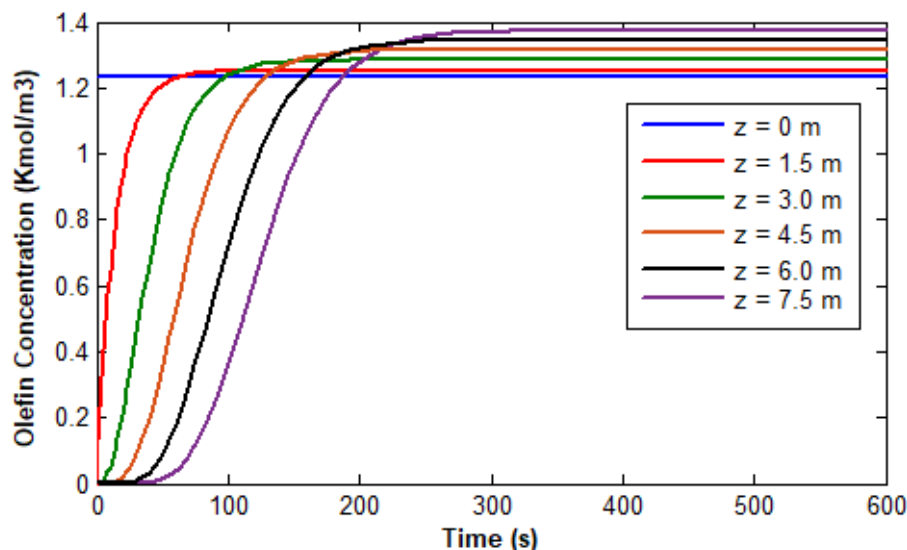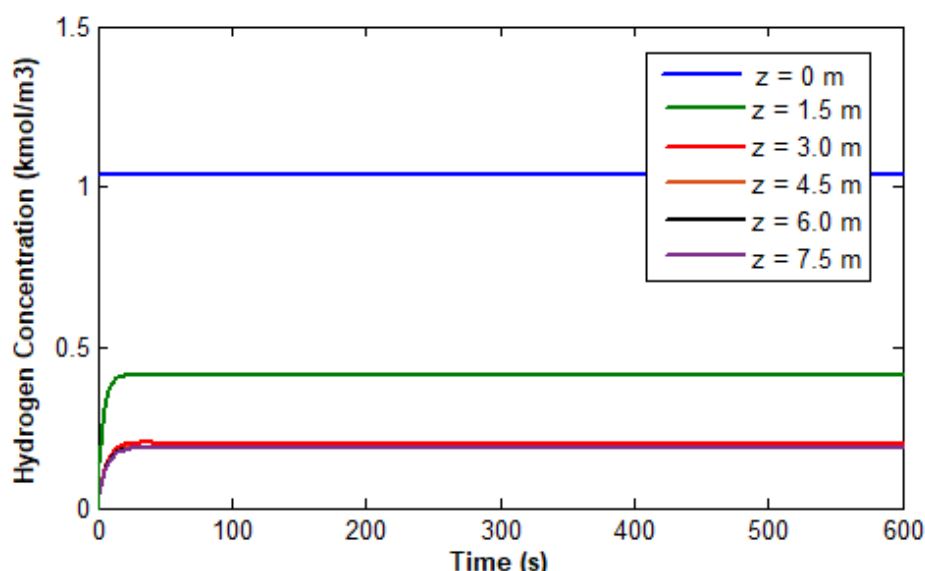
On the other hand, the olefin concentration, in Figure 3, reaches a steady-state level slower than the diolefin concentration, because the olefin is consumed by the reaction of the olefin saturation and produced at the same time by the reaction of the diolefin saturation. Furthermore, the reaction of diolefin hydrogenation is more effective than the reaction of olefin hydrogenation in the conditions applied to the studied reactor, since the diolefin hydrogenation is more reactive than the olefin hydrogenation reaction, as shown in Xin *et al*. (2018).

In Figure 5, it is shown the hydrogen liquid phase time-dependent concentration. Although the hydrogen concentration decreases tightly at the reactor inlet, the hydrogen concentration becomes stable after the first 3 meters. The substantial decrease at the catalytic bed inlet occurs because of the high reaction rate at the inlet of the bed, as shown in Mederos and Ancheyta (2007).

In Figure 6, the liquid-phase time-dependent temperature profile is shown. The steady state is reached simultaneously for the olefin concentration because the reaction of olefin saturation is exothermic, which contributes to the increase of the temperature along the

reactor. However, the olefin and diolefins saturation reactions are less exothermic than the hydrodesulfurization, hydrodenitrogenation, and hydrogenation of aromatics, which occurs significantly below 200 °C. Therefore, the temperature along the catalyst bed rises only 10 °C, which agrees with the experimental data used to develop the kinetic model. This result is consistent with the Dukanovic *et al.* (2013) study, which shows that the ΔT increase between 4 ºC and 12 °C in a hydrogenation reactor of gas oil blended with naphtha. It is pointed out that the increase of temperature along the catalytic bed occurs due to the reaction of olefin and diolefin saturation.

Figure 6 ▶
Dynamic profile of temperature along the reactor.
Source: research data
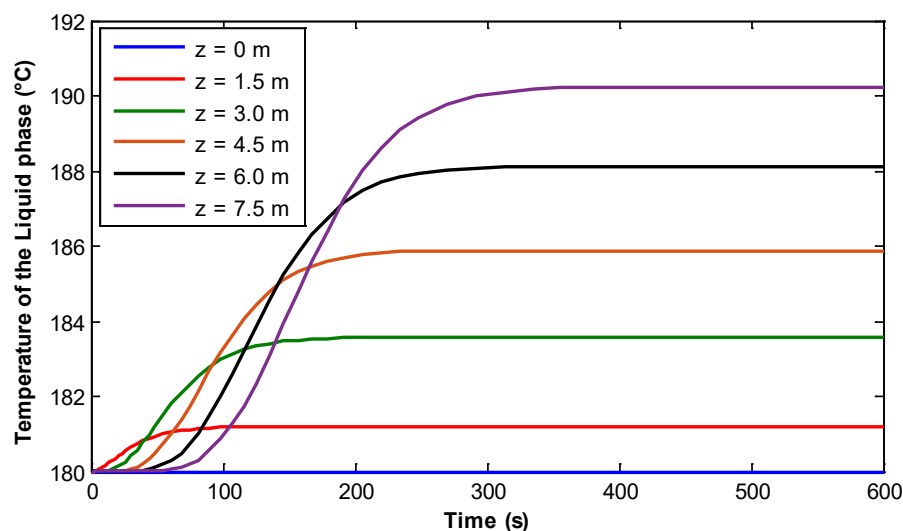
4 Conclusions

A one-dimensional heterogeneous mathematical model was employed in this work to obtain the kinetics of olefin and diolefin saturation reactions. The kinetic model, developed from industrial data obtained from a Brazilian refinery, was able to predict the temperature profile along the reactor length with absolute minimum error. The excellent agreement between the experimental results and those predicted by the developed model offers a reliability tool for simulations of other experiments. The model also can be used to develop advanced control strategies for the process. Regarding the concentration of olefins and diolefins, it was shown that the diolefin concentration decreased along the reactor while the olefin concentration increased.

Future works will study the effect of some input process variables (e.g., temperature, feed rate) on the reactor's concentration and temperature profile. It is also intended to investigate whether there are only two phases (solid and vapor) close to the reactor outlet.

Financing

Conflict of interest

The authors declare that there is no conflict of interest.

Nomenclature

$API°$	API gravity
a	dimensionless number of Glaso's correlation
a_L	gas-liquid interfacial area per unit reactor volume (1/cm)
a_S	liquid (or gas)-solid interfacial area per unit reactor volume (1/cm)
C_i	molar concentration of component i (mol/m³)
C_i^0	initial molar concentration of component i (mol/m³)
c_{P_i}	specific heat capacity of i phase (J/(kg.K))
d_c	catalyst diameter (m)
D_R	reactor diameter (m)
D_L^i	molecular diffusivity of compound i in the liquid phase (cm²/s)
e_j	activation energy of the j reaction (J/mol)
G_L	liquid superficial mass velocity (g/(cm² s))
h_{LS}	heat transfer coefficient for liquid-solid interface (J/(s cm² K))
H_{H_2}	henry's law coefficient of component i (MPa.cm³/mol)
k_j^i	mass transfer coefficient of component i at the interface j (cm/s)
k_j	reaction rate constant
LHSV	liquid hourly space velocity
L_T	length of catalyst bed (m)
P_T	reactor total pressure (MPa)
PM_{oil}	molecular weight (g/mol)
R	universal gas constant (J/(mol.K))
r_j	reaction rate j (mol/(kg.s))
T_0	inlet temperature (K)
T_{MBP}	mean average boiling point (K)
u_i	superficial velocity of i phase (cm/s)
Z	axial coordinate (m)

Greek letters

ε_i	hold up of i phase
ε_P	particle porosity
ϵ	bed void fraction

ρ_B	catalyst bulk density (g/cm³)
ρ_i	density at process conditions of i phase (g/cm³)
ρ_0	liquid density at standard conditions (15.6°C, 101.3kPa) (lb/ft³)
ρ_{20}	liquid density at 20°C (g/cm³)
v_c	critical specific volume of the gaseous components (cm³/mol)
v_i	molar volume of solute 'i' at its normal boiling temperature (cm³/mol)
v_c^m	critical specific volume (ft³/lb$_m$)
v_L	molar volume of solvent liquid at its normal boiling temperature (g/cm³)
v_N	molar gas volume at standard conditions (Nl/mol)
μ_L	absolute viscosity of the liquid (mPa s)
λ_i	solubility coefficient of the compound I (Nl/(MPa kg)

Subscripts

S	solid phase
L	liquid phase
G	gas phase
ol	olefin
dio	diolefin

References

ANCHEYTA, A. **Modeling and simulation of catalytic reactors for petroleum refining**. New Jersey: Wiley, 2011.

BADAWI, M.; VIVIER, L.; DUPREZ, D. Kinetic study of olefin hydrogenation on hydrotreating catalysts. **Journal of Molecular Catalysis A: Chemical,** v. 320, n. 1-2, p. 34-39, 2010. DOI: https://doi.org/10.1016/j.molcata.2009.12.012.

BHASKAR, M.; VALAVARASU, G.; SAIRAM, B.; BALARAMAN, K. S.; BALU, K. Three-phase reactor model to simulate the performance of pilot-plant and Industrial trickle-bed reactors sustaining hydrotreating reactions. **Industrial & Engineering Chemistry Research,** v. 43, n. 21, p. 6654-6669, 2004. DOI: https://doi.org/10.1021/ie049642b.

DUKANOVIC, Z.; GLISIC, S.; COBANIN, V.; NICIFOROVIC, M.; GEORGIOU, C.; ORLOVIC, A. Hydrotreating of straight-run gas oil blended with FCC naphtha and light cycle oil. **Fuel Processing Technology**, v. 106, p. 160-165, 2013. DOI: https://doi.org/10.1016/j.fuproc.2012.07.018.

JIMÉNEZ, F.; KAFAROV, V.; NUÑEZ, M. Modeling of industrial reactor for hydrotreating of vacuum gas oils: simultaneous hydrodesulfurization, hydrodenitrogenation, and hydrodearomatization reactions. **Chemical Engineering Journal**, v. 134, n. 1-3, p. 200-208, 2007. DOI: https://doi.org/10.1016/j.cej.2007.03.080.

KORSTEN, H.; HOFFMANN, U. Three-phase reactor model for hydrotreating in pilot trickle-bed reactors. **American Institute of Chemical Engineers Journal**, v. 42, n. 5, p. 1350-1360, 1996. DOI: https://doi.org/10.1002/aic.690420515.

LINDEN, R. **Algoritmos genéticos**. 3. ed. Rio de Janeiro: Ciência Moderna, 2012. In Portuguese.

MEDEROS, F. S.; ANCHEYTA, J. Mathematical modeling, and simulation of hydrotreating reactors: cocurrent versus countercurrent operations. **Applied Catalysis A: General**, v. 332, n. 1, p. 8-21, 2007. DOI: https://doi.org/10.1016/j.apcata.2007.07.028.

TOBA, M.; MIKI, Y.; MATSUI, T.; HARADA, M.; YOSHIMURA, Y. Reactivity of olefins in the hydrodesulfurization of FCC gasoline over CoMo sulfide catalyst. **Applied Catalysis B: Environmental**, v. 70, n. 1-4, p. 542-547, 2007. DOI: https://doi.org/10.1016/j.apcatb.2005.12.026.

TOLEDO, E. C. V.; MARIANO, A. P.; MORAIS, E. R.; STREMEL, D. P.; MEYER, J. F. C. A.; MACIEL FILHO, R. Development of rigorous and reduced heterogeneous dynamic models for fixed bed catalytic reactor and three-phase catalytic slurry reactor. **Chemical Product and Process Modeling**, v. 3, n. 1, p. 48, 2008. DOI: https://doi.org/10.2202/1934-2659.1256.

XIN, Q.; ALVAREZ-MAJMUTOV, A.; DETTMAN, H. D.; CHEN, J. Hydrogenation of olefins in bitumen-derived naphtha over a commercial hydrotreating catalyst. **Energy & Fuels**, v. 32, n. 5, p. 6167-6175, 2018. DOI: https://doi.org/10.1021/acs.energyfuels.8b00344.

YUI, S. Removing diolefins from coker naphtha necessary before hydrotreating. **Oil & Gas Journal**, v. 97, n. 36, p. 64-68, 1999. Available at: https://www.ogj.com/home/article/17229958/removing-diolefins-from-coker-naphtha-necessary-before-hydrotreating. Accessed on: 31 out. 2021.

YUI, S.; CHAN, E. Hydrogenation of coker naphtha with NiMo catalyst. **Studies in Surface Science and Catalysis**, v. 73, p. 59-66, 1992. DOI: https://doi.org/10.1016/S0167-2991(08)60797-1.